

Review of Beam Aided Diagnostics for ITER

M. von Hellermann¹, R.Jaspers¹, W.Biel², O.Neubauer², N.Hawkes³, Y. Kaschuck⁴, V.Serov⁴, S.Tugarinov⁴, D.Thomas⁵, W.Vliegthart⁶, and the ITPA Specialists Working Group on Beam-Aided Spectroscopy

¹FOM-Institute for Plasma Physics Rijnhuizen*, Association EURATOM, Netherlands, www.rijnh.nl; ²Institut für Plasmaphysik*, Forschungszentrum Jülich, Association EURATOM-FZJ, Germany, www.fz-juelich.de/ipp; ³UKAEA Culham Laboratory Euratom Association, Abingdon UK; ⁴TRINITI Troitsk, RF; ⁵General Atomics, San Diego, USA, ⁶TNO Science & Industries, Delft, NL, * Partners in the Trilateral Euregio Cluster

e-mail contact of main author: mgvh@rijnh.nl

Abstract A reassessment of the proposed package of beam aided diagnostic systems for ITER has led to a number of new developments. As a result of a joint development effort and comprehensive optimisation studies it was decided to use two separate diagnostic observation periscope assemblies both dedicated to CXRS (Charge Exchange Recombination Spectroscopy) and BES (Beam Emission Spectroscopy), which will exploit a Diagnostic Neutral Beam injected radially into the plasma:

A ‘Core CXRS’ system (EU) which covers dominantly the inner half of the confined plasma, and an ‘Edge CXRS’ system (RF) which ensures a high radial resolution in the outer half of the plasma. The Core system utilises an upper port periscope (U-port-3), and two periscopes located in an equatorial port (E-port-3) are envisaged for the Edge CX system. The equatorial port is shared with a dedicated MSE (Motional Stark Effect) system for the measurement of magnetic field pitch angles making use of the Heating Neutral Beams. A complementary MSE approach is proposed for the exploitation of intensity line ratios as measured by the BES data from upper and equatorial ports. More recently, at the 10th ITPA meeting on ITER diagnostics at Moscow in April 2006, it was proposed to share the use of Core and Edge periscopes with the new ITER partner India, and introduce a package of Beam related diagnostics in order to optimise instrumentation for CXRS and BES. The optical layouts of the two periscope systems have been recently reviewed and alignment and instrumentation schemes were developed.

A comprehensive multi-parameter spectral modelling effort based on an ITER reference scenario ($n_e(0)=10^{20}\text{m}^{-3}$, $T_e(0)=T_i(0)=20\text{keV}$, $B=5.2\text{T}$, $Z_{\text{eff}}=1.6$) the actual observation geometry, and modelling of atomic processes, has enabled an update of expected performances in terms of measurement accuracies, time and spatial resolution. Summarising the results of the performance study we can conclude that the measurement of radially resolved profiles of ion temperature, plasma rotation and ion densities, including that of the helium ash, are a realistic feasibility and expected parameter errors are compatible with the specifications laid down in the ITER “Measurement requirement table”. Moreover, spectral Signal-To-Noise numbers well above 10 are expected for the main part of the confined plasma, that is for $0.2 < r/a < 1$ for the Upper port and $0.4 < r/a < 1$ for the E-port.

1. Introduction

The main progress and development steps compared to earlier feasibility studies [1-6] can be summarised by the following features:

- 1) Relaxed operational constraints in terms of beam attenuation due to a reduced size of the ITER minor radius.
- 2) Significant signal boost thanks to the development of high-resolution and high optical throughput spectral instruments [6] and back illuminated high QE cameras linked to the decision to dedicate one spectral instrument for each radial channel.
- 3) Development of in-situ calibration procedures making use of beam-emission spectroscopy (BES), charge exchange spectroscopy (CXRS) and the simultaneous measurement of continuum radiation.
- 4) Development of suitable first-mirror schemes based on substantial progress in the understanding of erosion and depositions physics [7]. A re-allocation of the first mirror further inside the blanket structure (c.f. Figs.1 and 2) and a support structure

linked to a heat exchange system kept at 400C is believed to minimise erosion and deposition.

The need for a dual observation of the DNB path from upper and equatorial ports implying an overlap of observed DNB regions has been accepted as a key ingredient in the overall diagnostic performance analysis.

The main reasons for this proposed spatial extension of the viewing region of Core and Edge periscopes are an enhanced measurement capability for plasma rotation and the investigation of anisotropic features, e.g. alpha particle slowing-down features, or anisotropic ion temperatures in transient heating phases.

The issue of plasma rotation measurements which applies for both, “Core CXRS” and “Edge CXRS” periscopes is a challenging task. In the case of the Core CXRS periscope the measured Doppler shift represents both the velocity components of the dominant toroidal plasma rotation and that of the considerably smaller poloidal rotation. Although the main region for a significant poloidal rotation is expected close to the plasma boundary, or more generally, in the region of strong pressure gradients, independent poloidal rotation profiles as measured by the two equatorial edge CXRS periscopes (c.f. ref.1) are needed for a correction of the core profile. On the other hand, any poloidal rotation measurement will be flawed by gyro-orbit effects (ref.[8]), which potentially lead to systematic errors.

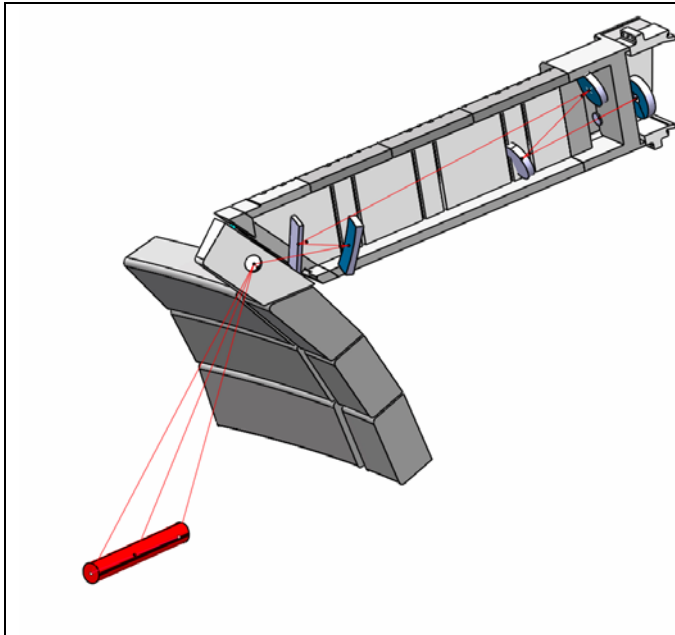


Fig.1 Schematic layout of Upper Port CXRS periscope with 100mm mono-crystal molybdenum ‘First-mirror’ in retracted position (400mm behind blanket surface). A two-leg labyrinth system reduces the neutron level by several orders of magnitudes. The coupling to a transfer fibre bundle is achieved by using Cassegrain optics. The system has been optimised for light collection and, equally important, for high image quality in the case of periscope alignment when laser light produced fibre spots will be used in connection with In-Vessel-Inspection-Cameras. The viewing area covers the entire DNB path between $0 < r/a < 1$.

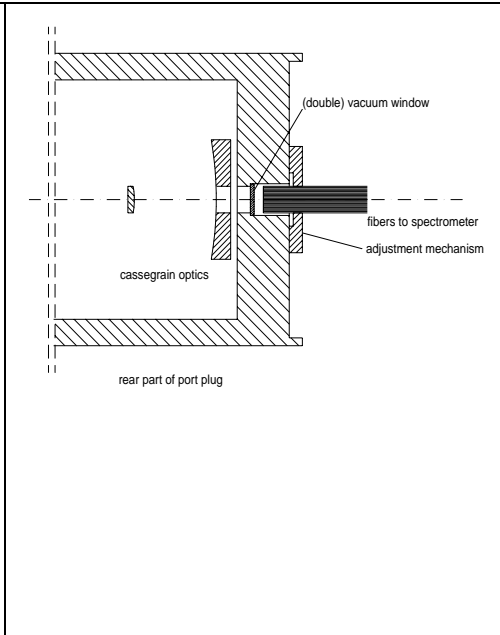


Fig.2 Schematic presentation of periscope Cassegrain coupling to receiving fibre bundle. The image of the rectangular array of fibres is matched to the DNB dimensions. Periscope magnification is 20:1 and a 2000mm x 240mm DNB area is imaged onto the fibres.

The gyro-orbit effect depends strongly on the observation geometry, and the combined evaluation of both upper and equatorial observation at the same radial points will improve the reliability of deduced velocity data. For this reason, the goal of aiming for a maximal overlap of the two observation periscope systems appeared to be highly desirable.

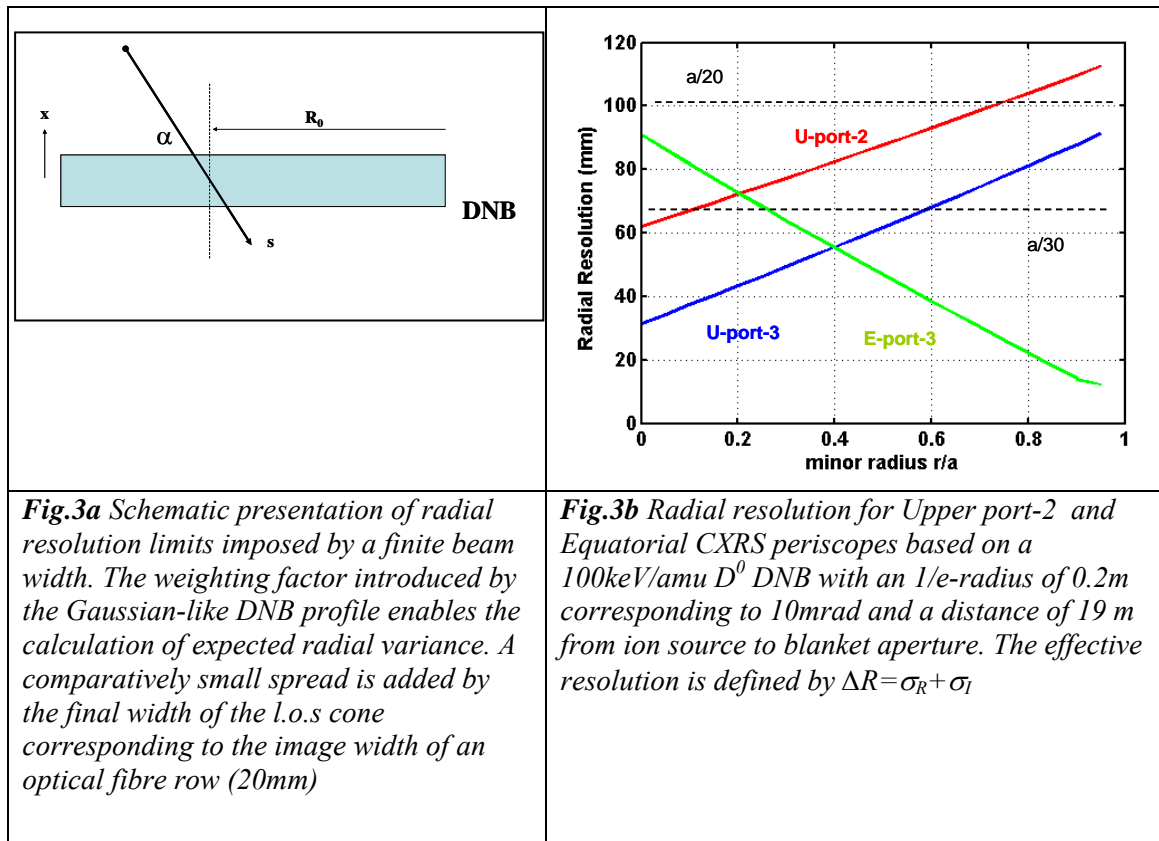
2.1 Radial Resolution issues

The effective radial resolution resulting from an oblique intersection of line of sight with a finite beam width can be expressed analytically in the case of a Gaussian-like beam shape with width w . Results for U- and E-ports are shown in Fig.3. A further reduction of the spatial spread imposed by blanket aperture which limits the effective DNB width inside the plasma region has not been taken into account.

$$\sigma_R^2 = \int_{-\infty}^{+\infty} ds (R - R_0)^2 \frac{1}{\sqrt{\pi}w} \exp\left[-\left(\frac{x(s)}{w}\right)^2\right]$$

$$\sigma'_R = w \cdot \text{abs}\left(\frac{\cot \alpha}{\sqrt{2} \cdot \sin \alpha}\right) + d_{\text{fib}} \cdot m \cdot \text{abs}\left(\frac{1}{2 \sin \alpha}\right)$$

Here the radius w denotes the 1/e radius of the DNB, d_{fib} , the fibre diameter, α the angle between line of sight and DNB and m the magnification factor of the optical system.



2.2 Modelling of Spectra and Performance analysis

The parametric simulation model allows the investigation of critical parameter dependencies encompassing beam parameters (beam energy, neutral current, species mix, beam divergence, viewing geometry (solid angles, line of sight directions, path length through plasma), spectral

instrumentation (optical throughput, spectral resolution, quantum efficiency, integration time), plasma data ($n_e, n_i, n_z, T_e, T_i, v_{rot}, B_t$) and modelled edge features (edge temperatures).

A similar exercise as for the thermal CX feature representing the dominant low-Z impurity ions has been performed for beam emission spectroscopy, with regard to local beam densities, pitch angles and Lorentz splitting as a measure of the total local field. The potential measurement of local fuel mixtures is investigated by a simulation of thermal CX spectra for deuterons and tritons.

Details of the Spectral modelling concept are described in ref. [9]. The main issue is that both **active** (beam induced) and **passive** features (continuum radiation, plasma edge line emission as well as passive charge exchange line emission) have to be quantitatively assessed. In theory, any passive background feature can be suppressed by beam-modulation. This recipe fails, however, in the case, when during the beam-on phase the neutral density background has changed compared to the beam-off phase. An alternative, or complementary, scheme is to implement an additional set of “passive” lines-of-sight which are directed to the immediate background close to the beam area (c.f. Fig.4) thus monitoring wall areas close to the active line of sight set, but avoiding direct light collection from the beam itself.

The figure of merit which represents the measurability of a CX spectrum in the presence of a dominant background of continuum radiation is given by the following expression for the SNR (c.f. ref [1]) ratio which takes into account a Gaussian-like intensity profile of the DNB, part of which is imaged onto the entrance slit of a spectrometer (Fig.5). The measured signal is the result of a 3-dim integration (see also Fig.4) along the line of sight and also across within the boundaries of the viewing cone. In the case of a limiting blanket aperture both integrations will be truncated within the blanket aperture boundaries.

$$I(\lambda = \lambda_{1/2}) = \frac{1}{2} \cdot \frac{1}{\sqrt{\pi} \cdot \lambda_d} \cdot \frac{1}{4\pi} \cdot n_z \cdot Q_z \cdot \int_{-r}^r dx \cdot \int_{\Delta z} dz \int_{l.o.s} ds \cdot n_b(x, y, z) \cdot \Delta\lambda$$

The Spectral-Signal to Noise (cf. ref.1) revised by the truncation of finite slit image and blanket aperture is defined by the ratio of spectral amplitude at half intensity divided by the underlying continuum noise level:

$$\frac{S}{N}(\lambda_{1/2}) = \frac{I_n c_\alpha \sigma_{CX} \exp\left\{-\int_z dr n_e \sum_z c_z \sigma_{z,stop}\right\}}{8\pi^2 \cdot \sin \alpha \cdot e \cdot \sqrt{Z_{eff} g_{ff} L_p B}} \cdot \sqrt{\Delta\tau \frac{\Delta\lambda \cdot \lambda_{de}}{\lambda_\alpha^2} \Delta\Omega_{obs} \cdot \Delta z \cdot \eta \cdot T / 2\Delta r}$$

$I_n = e \cdot n_{beam} \cdot v_{beam} \cdot A_{beam} = e \cdot n_{beam} \cdot v_{beam} \cdot \pi \cdot w_\perp^2$ neutral beam current (30A),

$c_\alpha = n_\alpha / n_e$: alpha particle concentration (0.04),

$\Delta\tau$ (sec): integration time (0.1s),

$\Delta\lambda$ (Å): instrument interval (2.5Å),

Δz : size of imaged slit along NB direction (20 mm)

Δr : half size of imaged slit across NB direction (120 mm)

ΔB_l : half size of blanket aperture width (150 mm)

λ_α (Å) = $\lambda_0 \sqrt{\frac{2T_i}{m_\alpha c^2}} = 3.42 \cdot T_i^{1/2}$ (keV) : Doppler width of the alpha particle spectrum,

λ_{de} (Å) = $\lambda_0 \sqrt{\frac{2T_e}{m_e c^2}} = 293 \cdot T_e^{1/2}$ (keV) : Doppler width corresponding to electron temperature,

L_p : path length of line of sight through plasma

η : quantum efficiency, $\eta=0.8$,
 t : optical transmission, $t=0.05$,
 ε : spectrometer étendue $\varepsilon=\Delta\Omega_{sp}\cdot A_{sp}=1.05\cdot 10^{-6}\text{ m}^2\text{sr}$.

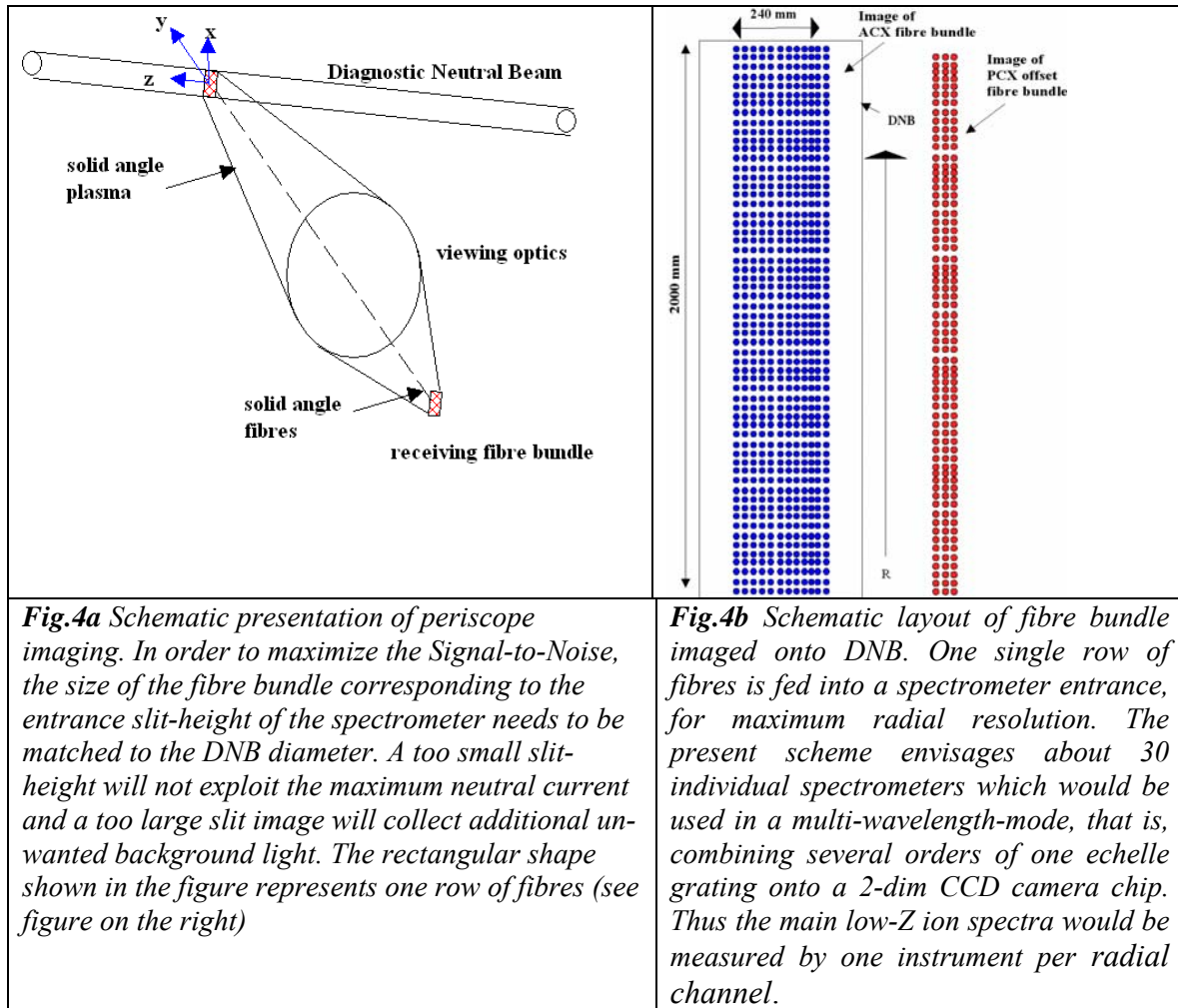


Fig.4a Schematic presentation of periscope imaging. In order to maximize the Signal-to-Noise, the size of the fibre bundle corresponding to the entrance slit-height of the spectrometer needs to be matched to the DNB diameter. A too small slit-height will not exploit the maximum neutral current and a too large slit image will collect additional unwanted background light. The rectangular shape shown in the figure represents one row of fibres (see figure on the right)

Fig.4b Schematic layout of fibre bundle imaged onto DNB. One single row of fibres is fed into a spectrometer entrance, for maximum radial resolution. The present scheme envisages about 30 individual spectrometers which would be used in a multi-wavelength-mode, that is, combining several orders of one echelle grating onto a 2-dim CCD camera chip. Thus the main low-Z ion spectra would be measured by one instrument per radial channel.

Two separate criteria must be satisfied, in order to demonstrate the projected measuring capabilities. The first is **spectral measuring capability** that is the unambiguous extraction of a CX spectrum, e.g. a HeII spectrum, in the presence of a huge background of continuum radiation and a multiplicity of plasma edge emission lines. The second criterion, which is listed in the ITER measurement requirement table is the expected **data accuracy** (c.f. Figs.5 and 7), i.e. experimental errors for ion temperature, plasma rotation and ion density. The first criterion is determined solely by the ratio of expected spectral CX signal, i.e. the amplitude at half maximum, and the fluctuation of underlying continuum radiation. The second criterion reflects the errors in the least-square fit of modelled spectral shapes to noisy experimental spectra. Ultimately, the quoted errors for the extracted physics parameter depend on the complexity of the spectral model, i.e. its degrees of freedom as well as the signal noise of the measured spectrum

The scenario for the performance study is summarised in the following:

Plasma data: $n_e(0) = 10^{20}\text{m}^{-3}$, $T_e(0)=T_i(0)=15\text{ keV}$, $v_{rot}=200\text{km/s}$, $B_{tor}=5.2\text{T}$

$R_0=6.2\text{m}$, $a=2\text{m}$, $\text{elongation}=1.6$

$c(\text{He}^{+2})=4\%$, $c(\text{C}^{+6})=1\%$, $c(\text{Be}^{+4})=2\%$ (with respect to electrons)

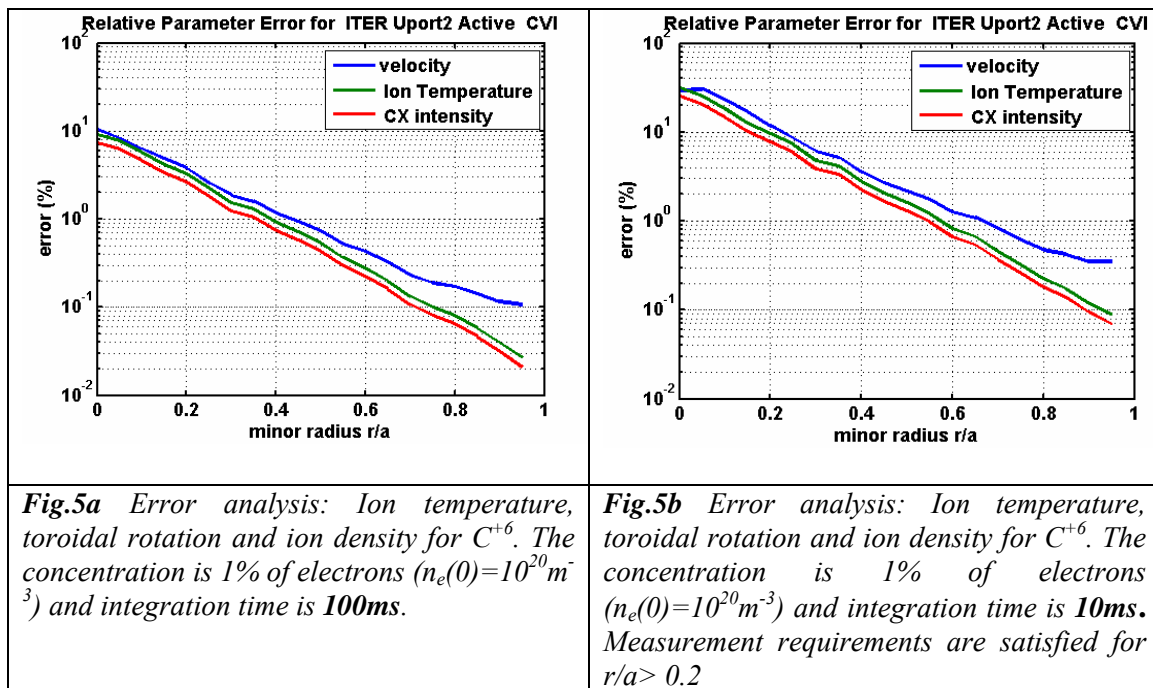
DNB¹ data: $P_{\text{NBI}}=6\text{MW}$, $E=100\text{ keV/amu}$, $I_{\text{neutral}}=30\text{A}$, used current for given optical configuration (and limitation by blanket cut) 62%

Optical link: 1200 PCS fibres of 1mm diameter, length 120m, overall transmission including spectrometer grating : $T_{\text{total}}=0.05$.

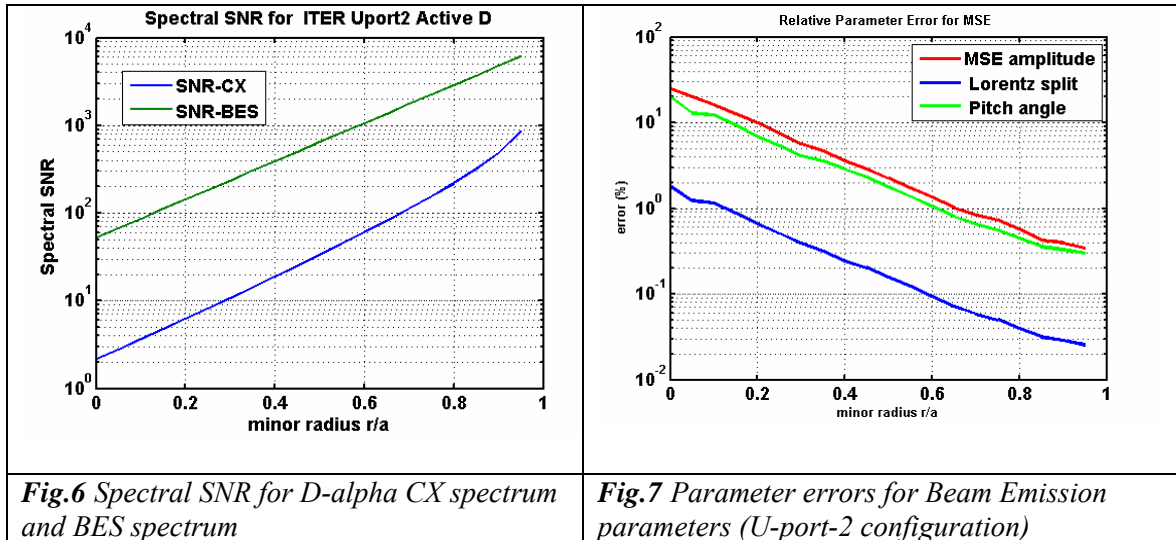
The transmission estimate T is based on the periscope losses (first mirror: 0.5, followed by 4 dielectric mirrors: 0.95^4 , double window: 0.92^2 , 120m fibre link: 0.02db/m @ 500nm: 0.7, fibre F-number change: 0.5, input optics : 0.92, grating efficiency: 0.6)

Instrumentation:

High-through-put, high-resolution spectrometers: Echelle Littrow configuration, F/3, $f=600\text{mm}$, slit-width = 1mm, slit-height = 12mm, dispersion = 2.6 A/mm. The enhanced slit height of 12mm is adapted to the 10mrad DNB diameter of 240mm.



¹ The update of DNB specification represents the status following discussion with members of the Indian Institute for Plasma Research, Bhat, Gandhinagar, who as new ITER partners have taken on the task for DNB development in 2006. The main changes compared to earlier specifications are a higher total neutral current (30A compared to 22A), and at the same time a lower current density (higher beam divergence (10mrad compared to 5mrad). The size of blanket-cut aperture for the DNB inlet is presently under discussion, also a possible toroidal tilt of the DNB by a few degrees to avoid stagnating fast ions as expected in the case of a purely radial injection.



3. Future CXRS and BES work

Supporting pilot experiments and activities are currently discussed or are already implemented. Specific goals are: optimisation of spectral instrumentation, feasibility of a Motional Stark Effect evaluation based on line ratios, ‘first-mirror’ test-bed experiments at the tokamak TEXTOR. The detection boost factor moving, for example, from the present JET CXRS system (several radial channels measured by one common spectrometer and CCD camera) to the envisaged ITER system (one spectrometer per radial channel) is about two orders of magnitude. For this reason it appeared sensible to explore in a pilot experiment in a look-alike viewing configuration and instrumentation the noise and detection performance. The following table shows the expected detection sensitivity (CCD photo-electrons per emitted photon flux) for the JET, ITER and the presently implemented pilot experiment on TEXTOR.

	JET	ITER(predicted)	TEXTOR-Pilot
Quantum efficiency (%)	50	80	80
Slit width (mm)	0.8	1.0	0.6
Slit height(mm)	1.0	12.0	6.3
F-number	10	3	3
Etendue (sr·m ²)	$5.2 \cdot 10^{-9}$	$1.05 \cdot 10^{-6}$	$3.3 \cdot 10^{-7}$
transmission	0.05	0.05	0.07
Responsivity \mathfrak{R} (pe/(ph·m ⁻² ·sr ⁻¹))	$1.3 \cdot 10^{-10}$	$4.2 \cdot 10^{-8}$	$1.8 \cdot 10^{-8}$

Conclusions

Significant progress has been made in terms of conceptual layout of the observation periscopes optical design and instrumentation for CXRS and BES. Advanced modelling in context with existing CXRS diagnostic systems at JET, TEXTOR, ASDEX-UG and Tore

Supra has enabled more precise predictions for active and passive spectral features. A performance analysis based on synthetic spectra has demonstrated the feasibility of the ITER CXRS and BES diagnostic with accuracies, radial and temporal resolution in line of the specification of the ITER measurement requirement table.

References

- [1] M.von Hellermann “Active Charge Exchange Spectroscopy (CXRS) and Beam Emission Spectroscopy (BES+MSE) with Diagnostic Neutral Beam (DNB)” (EFDA contract: 01.649, 2003; not publicly available, contact: mgvh@rijnh.nl)
- [2] M. von Hellermann et al., “Feasibility of Quantitative Spectroscopy on ITER”, ‘Diagnostics for Experimental Fusion Reactors I’, Plenum Press N.Y. 1996, Ed. P.E.Stott et al., page 321
- [3] Thomas, D.M., Burrell, K.H., Wade, M.R., Snider, R.T., “Prospects for Core Helium Density and Related Measurements on ITER Using Active Charge Exchange”, ‘Diagnostics for Experimental Thermonuclear Fusion Reactors II’, Ed. P.Stott et al., Plenum Press, New York (1998) p. 361-370
- [4]Thomas, D.M., Burrell, K.H., Wade, M.R., Snider, R.T., “Prospects for Charge-Exchange Recombination-Based Measurements on ITER Using a He^o Diagnostic Neutral Beam”, 12th Topical Conference on High Temperature Plasma Diagnostics, Princeton, New Jersey, United States, *Rev. Sci. Instrum.* 70, 886-889 (1999)
- [5]A. Malaquias, M. von. Hellermann, S. Tugarinov, P. Lotte, N. Hawkes, M. Kuldkepp, E. Rachlew, A. Gorshkov, C. Walker, A. Costley, G. Vayakis, “Active beam spectroscopy diagnostics for ITER: Present status”, 15th Topical Conference on High Temperature Plasma Diagnostics, San Diego, California, United States, *Rev. Sci. Instrum.*, vol.75, no. 10, pp. 3393-3398, October 2004.
- [6] S.Tugarinov, A.Krasilnikov,V.Dokouka, R.Khayrutidinov, I.Beigman, I.Tolstikhina, L.Vainshtein, M von Hellermann, A.Malaquias, “Conceptual Design of the CXRS Diagnostic for ITER”, *Rev.Sci.Instr.* 74,2075(2003)
- [7] K.Vukolov , V. Voitsenya, “Report of the First Mirror Working Group”
6th Meeting of the ITPA Topical Group on Diagnostics Part I, Naka, February 2004
- [8] “ New Understanding of Poloidal Rotation Measurements”, R.E. Bell, M.C. Zarnstorff, E.J. Synakowski, Joint European-US Transport Task Force Workshop , Portland, Oregon, April 1999
- [9] “ Status of the DNB based ITER CXRS and BES diagnostic”, M.von Hellermann, R.Jaspers, W.Biel, A.Litnovsky, O.Neubauer, M.Pap, N.C.Hawkes, C.Marren, B.Walton, Y. Kaschuck, V.Serov, S.Tugarinov, W.Vliegthart, K.Moddemeijer, C.Walker, C.Ingesson, 16th Topical Conference on High Temperature Plasma Diagnostics, Williamsburg, New Jersey, United States, *Rev. Sci. Instrum.*, vol.77, 2006